

Effect of Surface Functionalization of MCM-41-Type Mesoporous Silica Nanoparticles on the Endocytosis by Human Cancer Cells

Igor Slowing, Brian G. Trewyn, and Victor S.-Y. Lin*

Department of Chemistry, Iowa State University, Ames, Iowa 50011-3111

Received June 28, 2006; Revised Manuscript Received September 28, 2006; E-mail: vsylin@iastate.edu

Recent studies on the interaction between surface-functionalized inorganic nanoparticles and animal cells have shown great potential for utilizing these size-defined nanomaterials for various biomedical and biotechnological applications, such as cell type recognition, disease diagnosis, intracellular imaging, and drug/gene delivery. In particular, several recent reports,^{1–5} including our own studies, have shown that mesoporous silica nanoparticles can be efficiently endocytosed by mammalian cells. The large surface areas and pore volumes of these materials offer the possibility of encapsulating and delivering large quantities of biogenic molecules through different cell membranes and to various intracellular targets. Furthermore, it has been demonstrated recently that the mesopores of these nanoparticles can be closed and opened at will by various capping/release strategies.^{1,3,6} These new breakthroughs make the surface-functionalized MSNs excellent candidates for intracellular controlled-release delivery. To realize this goal, an important prerequisite would be to understand the mechanism of cellular uptake of these surface-functionalized mesoporous silica nanoparticles, so that the uptake of MSNs by different cell types can be regulated. For example, to use these MSNs as efficient intracellular delivery vehicles it would be important to use different surface functional groups to manipulate the rate of escape of MSNs from endosomes to cytosol and other intracellular organelles. To the best of our knowledge, no report has examined the effect of surface functional groups on the cellular uptake properties of these mesoporous silica-based nanoparticles. Herein, we report on the synthesis of a series of organically functionalized MSNs and investigate the mechanism and efficiency of endocytosis of these materials with different charge profiles on human cervical cancer cells (HeLa).

First, we synthesized a fluorescein-functionalized, MCM-41-type mesoporous silica nanoparticle material (FITC-MSN).⁷ As shown in Figure 1, FITC-MSN has an average particle diameter of 150 nm. The MCM-41-type mesoporous structure with a 2.4 nm average pore diameter and a surface area of 850 m²/g was confirmed by powder X-ray diffraction (XRD), nitrogen sorption isotherms, and scanning and transmission electron microscopy (SEM and TEM, respectively) measurements.⁷ Three functional groups, 3-aminopropyl (AP), *N*-(2-aminoethyl)-3-aminopropyl (AEAP), and *N*-folate-3-aminopropyl (FAP), were grafted onto the external surface of the FITC-MSN by refluxing 6 mmol of the corresponding trimethoxysilyl derivatives with 1 g of FITC-MSN in toluene for 20 h. The amino groups of the 3-aminopropyl and the *N*-(2-aminoethyl)-3-aminopropyl were transformed into guanidinopropyl (GP) and 3-[*N*-(2-guanidinoethyl)guanidino]propyl (GEGP) groups, respectively, via a literature procedure.⁸ The amount of surface-anchored AP, GP, GEGP, and FAP groups were determined by solid-state direct polarization ²⁹Si NMR to be 1.5, 1.3, 0.97, and 0.89 mmol/g, respectively. After the grafting of these groups, the surfactant template (CTAB) molecules were removed from the MSNs by refluxing 1.0 g of the materials in 100 mL of methanol and 1 mL of concentrated HCl.

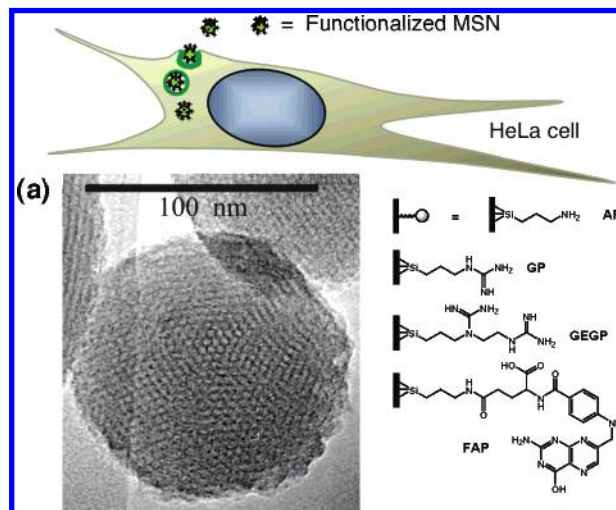


Figure 1. Schematic representation of the endocytosis of organically functionalized mesoporous silica nanoparticles (MSNs) by a human cervical cancer cell (HeLa). (a) TEM image of a fluorescein-functionalized MSN (FITC-MSN).

Table 1. ζ -Potentials and ED₅₀ for Cellular Uptake of the MSNs

| material | ζ -potential [mV] | ED ₅₀ (μ g/mL) |
|----------|-------------------------|--------------------------------|
| FITC-MSN | -34.73 ± 3.50 | 12.35 |
| AP-MSN | -4.68 ± 1.54 | 10.95 |
| GP-MSN | -3.25 ± 0.275 | 8.8 |
| GEGP-MSN | $+0.57 \pm 0.095$ | 6.39 |
| FAP-MSN | $+12.81 \pm 1.60$ | 2.73 |

In contrast to the zeta potential (ζ -potential) of -34.73 mV for FITC-MSN, the values of ζ -potential for AP-, GP-, GEGP-, and FAP-functionalized FITC-MSNs in 100 mM PBS buffer (pH 7.4) increased positively from -4.68 to $+12.81$ mV, respectively, as outlined in Table 1.

To examine the biocompatibility of MSNs, we compared the cell growth profiles of HeLa cultures with and without MSNs (0.1 mg/mL) for 4 days. Our results showed no difference in growth with or without the MSNs.⁷

To investigate the uptake of these organically functionalized MSNs, different concentrations of MSNs were introduced to HeLa cell cultures seeded at 1.0×10^5 cells/mL for 10 h in serum-free media. The degree of endocytosis was determined by quantifying live cells that exhibited green fluorescence with flow cytometry. To ensure the fluorescence observed in the flow cytometry measurements was indeed from the MSNs that have been endocytosed, a fluorescence quencher, Trypan Blue, was included in the cell suspension. Since Trypan Blue cannot penetrate the membranes of living cells, it could only quench the fluorescence of those MSNs that are adsorbed on the exterior surface of cells.⁹ The plots of the logarithms of the concentrations of MSNs versus the percentages of cells that took up the MSNs showed a sigmoidal behavior, which

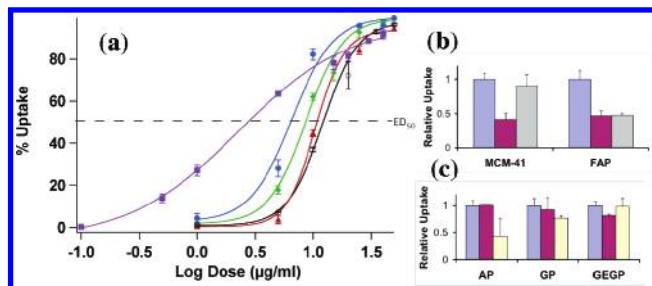


Figure 2. (a) Uptake of the synthesized MSNs as a function of their concentration: (○) FITC-, (▲) AP-, (◆) GP-, (●) GEGP-, and (■) FAP-MSNs. (b) and (c) Uptake of the materials in absence (blue bars) and presence of a series of inhibitors: 450 mM sucrose (prune); 1 mM folic acid (gray); 200 mM genistein (cream).

is typical of dose–response endocytosis (Figure 2a). The degrees of uptake of these MSNs were determined by their ED_{50} values.

The uptake of nonfunctionalized, negatively charged silica materials by cells has been found to occur through a nonspecific adsorptive endocytosis,⁵ and the resting potentials of cell membranes are normally negative (-50 mV for HeLa).¹⁰ The relationship between the ED_{50} values and the ζ -potentials of these surface-functionalized MSNs is summarized in Table 1. Flow cytometry results suggested that the endocytosis of MSN could be manipulated by different surface functionalization. In addition to the surface charge effect, it is well-known that the membranes of human cancer cells are abundant with folate receptors.¹¹ The folate groups on FAP-MSN could also play an active role in facilitating a receptor-mediated endocytosis.

To investigate the possible mechanism of endocytosis of the different MSNs, we tested the cellular uptake of these materials in presence of specific inhibitors. Our results indicated that only the FITC- and FAP-MSNs are endocytosed via a clathrin-pitted mechanism, as the uptakes were inhibited by 450 mM sucrose (Figure 2b,c). In addition, the uptake of FAP-MSN was partially inhibited in presence of 1 mM folic acid, whereas the endocytosis of FITC-MSN was not perturbed (Figure 2b). This observation along with the higher uptake observed for FAP-MSN suggests that the mechanism of endocytosis for this material is mediated by folic acid receptors on the HeLa cell surface. In contrast, the endocytosis of AP- and GP-MSNs was affected by a caveolar inhibitor, genistein (Figure 2c), suggesting that these materials are endocytosed via a caveolae-mediated mechanism. The uptake mechanism of GEGP remains unclear because the endocytosis was not dramatically affected by any of the inhibitors.

To study the impact of surface functionality in endosome escape, we stained the endosomes with a red fluorescent endosome marker (FM 4-64) and monitored the confocal fluorescence micrographs (Figure 3)⁷ of FITC-MSNs with different functional groups in HeLa cells. The green fluorescent spots in Figure 3a represent the FITC-MSNs that were able to escape the endosomes, whereas those that were trapped inside the vesicles are yellow in color, which is the result of overlapping red (endosome) and green (MSN) spots. We found that the more negatively charged FITC- and AP-MSNs appeared to be able to escape from endosomes within 6 h, while those with more positive ζ -potentials, such as GP-, GEGP- and FAP-MSNs, remained trapped within endosomes.⁷ This behavior

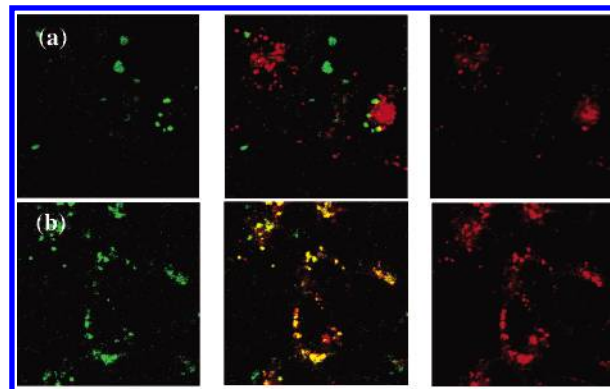


Figure 3. Confocal fluorescence images of HeLa cells stained with FM 4-64 and 40 $\mu\text{g/mL}$ suspensions of (a) FITC-MSN and (b) FAP-MSN after 6 h of introduction. The fluorescent images (left) show the MSNs (green) and FM 4-64-labeled endosomes (red). The corresponding phase contrast images are displayed on the right.

could be attributed to the Proton Sponge effect,¹² where the more negatively charged materials would have a better buffering capacity, which is important for the endosome escape.¹²

In conclusion, we have demonstrated the uptake of MCM-41-type mesoporous silica nanoparticles by HeLa cells can be regulated by different surface functionalization. Our results indicated that these surface functionalities could also affect MSN's ability to escape endosomal entrapment, which is a key factor in designing effective intracellular delivery vehicles.

Acknowledgment. This research was supported by the NSF (CHE-0239570). We thank the cell and hybridoma facility of ISU for their assistance.

Supporting Information Available: Syntheses and characterizations of MSNs, cell cultures, flow cytometry, confocal fluorescence microscopy, and immunochemistry experiments. This material is available free of charge via the Internet at <http://pubs.acs.org>.

References

- (1) Giri, S.; Trewyn, B. G.; Stellmaker, M. P.; Lin, V. S. Y. *Angew. Chem., Int. Ed.* **2005**, *44*, 5038–5044.
- (2) Huang, D.-M.; Hung, Y.; Ko, B.-S.; Hsu, S.-C.; Chen, W.-H.; Chien, C.-L.; Tsai, C.-P.; Kuo, C.-T.; Kang, J.-C.; Yang, C.-S.; Mou, C.-Y.; Chen, Y.-C. *FASEB J.* **2005**, *19*, 2014–2016.
- (3) Lai, C.-Y.; Trewyn, B. G.; Jeftinija, D. M.; Jeftinija, K.; Xu, S.; Jeftinija, S.; Lin, V. S. Y. *J. Am. Chem. Soc.* **2003**, *125*, 4451–4459.
- (4) Lin, Y.-S.; Tsai, C.-P.; Huang, H.-Y.; Kuo, C.-T.; Hung, Y.; Huang, D.-M.; Chen, Y.-C.; Mou, C.-Y. *Chem. Mater.* **2005**, *17*, 4570–4573.
- (5) Xing, X.; He, X.; Peng, J.; Wang, K.; Tan, W. *J. Nanosci. Nanotechnol.* **2005**, *5*, 1688–1693.
- (6) Gruenhagen, J. A.; Lai, C.-Y.; Radu, D. R.; Lin, V. S. Y.; Yeung, E. S. *Appl. Spectrosc.* **2005**, *59*, 424–431.
- (7) See Supporting Information.
- (8) Bernatowicz, M. S.; Youling, W.; Matsueda, G. R. *J. Org. Chem.* **1992**, *57*, 2497–2502.
- (9) Hed, J.; Hallden, G.; Johansson, S. G.; Larsson, P. *J. Immunol. Methods* **1987**, *101*, 119–125.
- (10) Szabo, I.; Brutsche, S.; Tombola, F.; Moschioni, M.; Satin, B.; Telford, J. L.; Rappuoli, R.; Montecucco, C.; Papini, E.; Zoratti, M. *EMBO J.* **1999**, *18*, 5517–5527.
- (11) Ladino, C. A.; Chari, R. V. J.; Bourret, L. A.; Kedersha, N. L.; Goldmacher, V. S. *Int. J. Cancer* **1997**, *73*, 859–864.
- (12) Boussif, O.; Lezoualc'h, F.; Zanta, M. A.; Mergny, M. D.; Scherman, D.; Demeneix, B.; Behr, J.-P. *Proc. Natl. Acad. Sci. U.S.A.* **1995**, *92*, 7297–7301.

JA0645943

Supporting Information

Effect of Surface Functionalization of MCM-41 Type Mesoporous Silica Nanoparticles on the Endocytosis by Human Cancer Cells

Igor Slowing, Brian G.Trewyn, and Victor S.-Y. Lin*

Department of Chemistry, Iowa State University, Ames, Iowa 50011-3111

E-Mail: vsylin@iastate.edu

1. Experimental:

1.1. Materials

Tetraethylorthosilicate was purchased from Gelest. 3-aminopropyltrimethoxysilane, 3-[*N*-(2-aminoethyl)amino]propyltrimethoxysilane, fluorescein isothiocyanate isomer I, folic acid, 1-*H*-pyrazole carboxamide hydrochloride, diisopropyl ethylamine, and *N*-ethyl-*N*-(3-dimethylaminopropyl)carbodiimide hydrochloride were purchased from Aldrich. All chemicals were used as received.

1.2. Synthesis of fluorescein isothiocyanate-labeled mesoporous silica nanoparticles (FITC-MSNs)

FITC-MSN was prepared by reacting 500 mg (1.11 mmol) of fluorescein isothiocyanate with 0.2 mL (1.15 mmol) of (3-aminopropyl)trimethoxysilane (APTMS) for 2 h. The resulting product was introduced to a co-condensation reaction of 10.0 mL (43.9 mmol) tetraethylorthosilicate (TEOS), 2.04 g (5.32 mmol) cetyltrimethylammonium bromide (CTAB), 960 mL water, and 7.0 mL sodium hydroxide (2 M). The reaction mixture was heated at 80 °C, under vigorous stirring for 2 h. The resulting orange colored solid was filtered, washed thoroughly with methanol and dried under vacuum for 20 h.

1.3. Synthesis of trimethoxysilylated FAP precursor (FAPTMS)

Following a literature procedure,¹ folic acid (66 mg, 0.15 mmol) was mixed with 150 mg (0.94 mmol) of *N*-ethyl-*N*'(3-dimethylaminopropyl)carbodiimide hydrochloride (EDC) in 10 mL of dimethylsulfoxide. After 30 minutes of stirring, APTMS (30 μ L, 0.17 mmol) was added to the solution. The reaction was stirred at room temperature for 4 h. To avoid undesired hydrolysis of the FAPTMS, the DMSO solution was directly used for the grafting reaction described below without purification.

1.4. Synthesis of surface functionalized FITC-MSNs

3-Aminopropyl (AP), 3-[*N*-(2-aminoethyl)amino]propyl (AEAP), and 3-(*N*-folateamino)propyl (FAP) functionalized FITC-MSNs were prepared by grafting 6 mmol of the trimethoxysilylated precursors,

1. Leamon, C.P.; Low, P.S. *Proc. Natl. Acad. Sci. USA* **1991**, 88, 5572-5576.

APTMS, AEAPTMS (both were purchased from Aldrich), and the aforementioned FAPTMS, respectively, to the surface of FITC-MSN (1 g) in refluxing toluene (100 mL) for 20 h. The resulting materials were filtered, washed with methanol and dried under vacuum for 20 h. The success of the surface functionalization and the quantification of organic groups were examined by solid-state ^{13}C and ^{29}Si NMR spectroscopy (Section 2.4).

1.5. Removal of the CTAB surfactant from the organically functionalized FITC-MSNs

The CTAB surfactant was removed from each of the aforementioned materials by heating the mixture of 1.0 g of the MSN material in 100 mL of methanol and 1.0 mL of concentrated hydrochloric acid for 6 h at 60 °C. The surfactant-removed materials were centrifuged, washed several times with methanol and dried under vacuum for 20 h.

1.6. Synthesis of GP- and GEGP-functionalized FITC-MSNs

GP-functionalized FITC-MSN: 3-Guanidiniopropyl (GP) derivatized FITC-MSN was prepared by stirring 0.5 g of the surfactant-removed AP-MSN with 0.3 g (2.0 mmol) of 1-*H*-pyrazole carboxamidine hydrochloride (HPCA), 0.36 mL (2.1 mmol) diisopropyl ethylamine in 5 mL of dimethylformamide (DMF) for 24 h. The resulting material was centrifuged, washed with methanol and dried under vacuum for 20 h.

GEGP-functionalized FITC-MSN: 3-[*N*-(2-guanidinioethyl)guanidinio]propyl (GEGP) derivatized FITC-MSN was prepared by stirring 0.5 g of the surfactant-removed AEAP-MSN with 0.6g (4.0 mmol) of 1-*H*-pyrazole carboxamidine hydrochloride (HPCA), 0.72 mL (4.1 mmol) diisopropyl ethylamine in 5 mL of dimethylformamide (DMF) for 24 h. The resulting material was centrifuged, washed with methanol and dried under vacuum for 20 h.

2. Characterizations

2.1. Nitrogen adsorption/desorption isotherms

Surface analysis of the materials was performed by nitrogen sorption isotherms in a Micromeritics ASAP2000 sorptometer. The surface areas were calculated by the Brunauer-Emmett-Teller (BET) and the pore size distribution were calculated by the Barrett-Joyner-Halenda method.

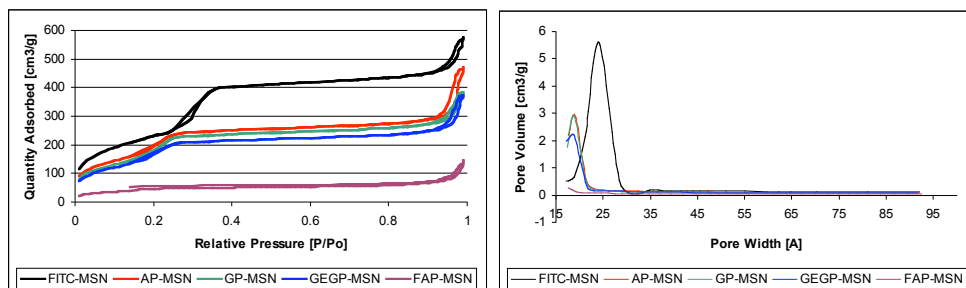


Figure S1. BET nitrogen adsorption/desorption isotherms (left), and BJH pore size distribution (right) of the MSN materials.

Table S1. Surface properties of the MSN materials

| Material | BET Surface Area | Average Pore Width [Å] | Pore Volume |
|----------|------------------|------------------------|-------------|
| | [m²/g] | | [cm³/g] |
| FITC-MSN | 850 | 24 | 0.799 |
| AP-MSN | 706 | 19 | 0.636 |
| GP-MSN | 645 | 19 | 0.570 |
| GEGP-MSN | 623 | 19 | 0.522 |
| FAP-MSN | 177 | <17 | 0.195 |

2.2. Powder X-ray diffraction

X-ray diffraction patterns were obtained in a Scintag XDS-2000 powder diffractometer using Cu K α irradiation. All of the materials exhibit the hexagonal mesoporous structure, which is typical of MCM-41 with the characteristic (100) peak between 2.10 and 2.20 degrees (2 θ). The high ordered (110) and (200) peaks are also observed in these organically functionalized FITC-MSNs.

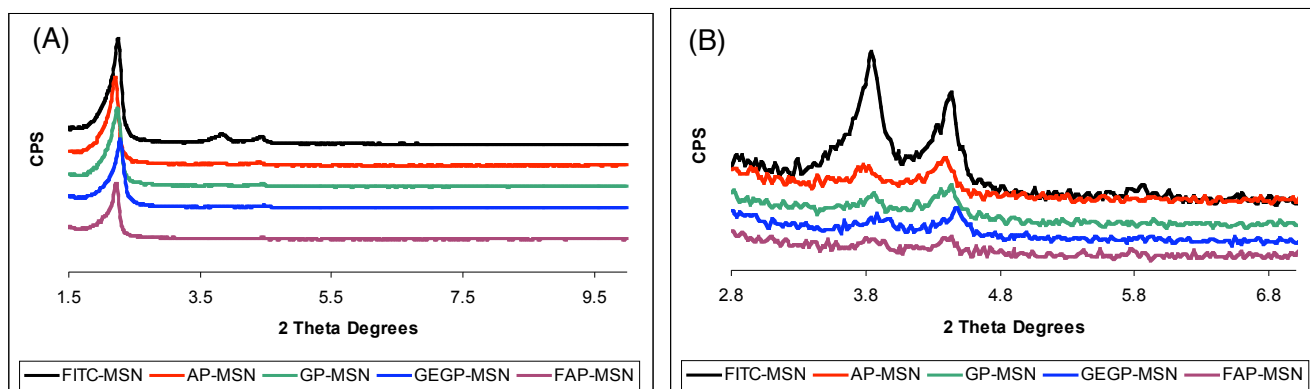


Figure S2. (A) The X-Ray diffraction patterns of the prepared materials from 1.5 to 10 degrees (2θ). (B) Enlarged view of the (110) and (200) peaks between 2.7 and 7.0 degrees (2θ).

2.3. ζ -Potential measurement

The ζ -potentials of these MSN materials were measured in a Malvern Nano HT Zetasizer. Each material was tested in triplicate. Suspensions ($200 \mu\text{g/mL}$) of each material in PBS buffer were prepared. The pH of the PBS buffer was 7.69 (40 mg KCl, 40 mg KH_2PO_4 , 1.600g NaCl and 0.432g $\text{Na}_2\text{HPO}_4 \cdot 7\text{H}_2\text{O}$ per liter of nanopure water.) The ζ -potential was measured immediately after ultrasonication for 15 min. For the ζ -potential measurements of FITC-, AP- and FAP-MSN, 30 scans were taken per sample, while for the ζ -potential measurement of GP- and GEGP-MSN, the number of scans was reduced to 10 to avoid any deposition of the GP- and GEGP-MSNs on the surface of electrodes. Figure S3 shows zeta-potential graphs.

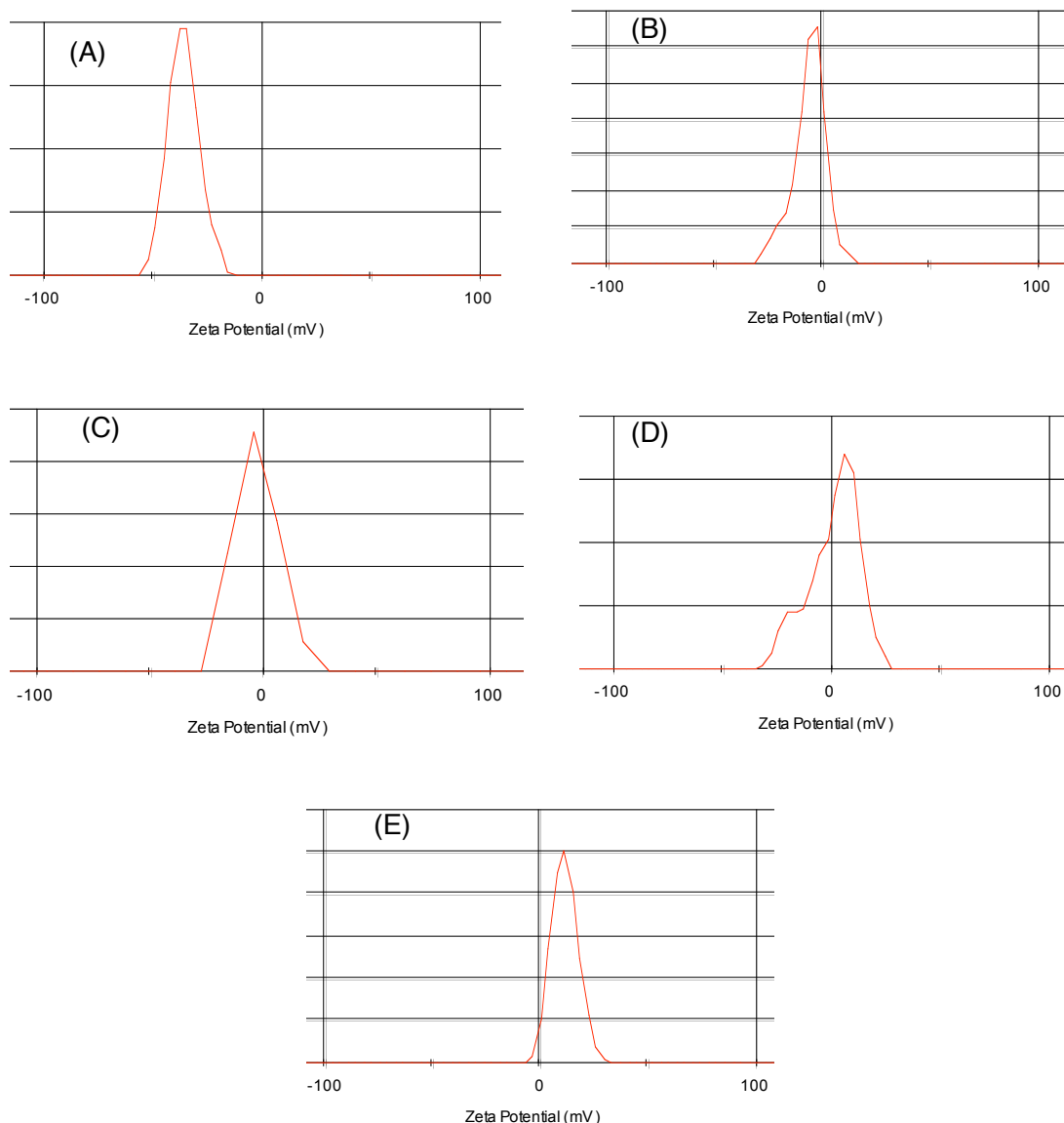


Figure S3. ζ -potential graphs of (A) FITC-MSN, (B) AP-MSN, (C) GP-MSN, (D) GEGP-MSN, and (E) FAP-MSN in 10 mM PBS buffer pH 7.69.

2.4. Solid state NMR

Solid-state ^{13}C and ^{29}Si crossed polarization and direct polarization magic angle spinning NMR (CP- and DP-MAS NMR) measurements of MSNs were conducted by using a Bruker MSL-300 spectrometer with a Bruker 4 mm rotor MAS probe.

2.4.1. MAS ^{13}C -NMR

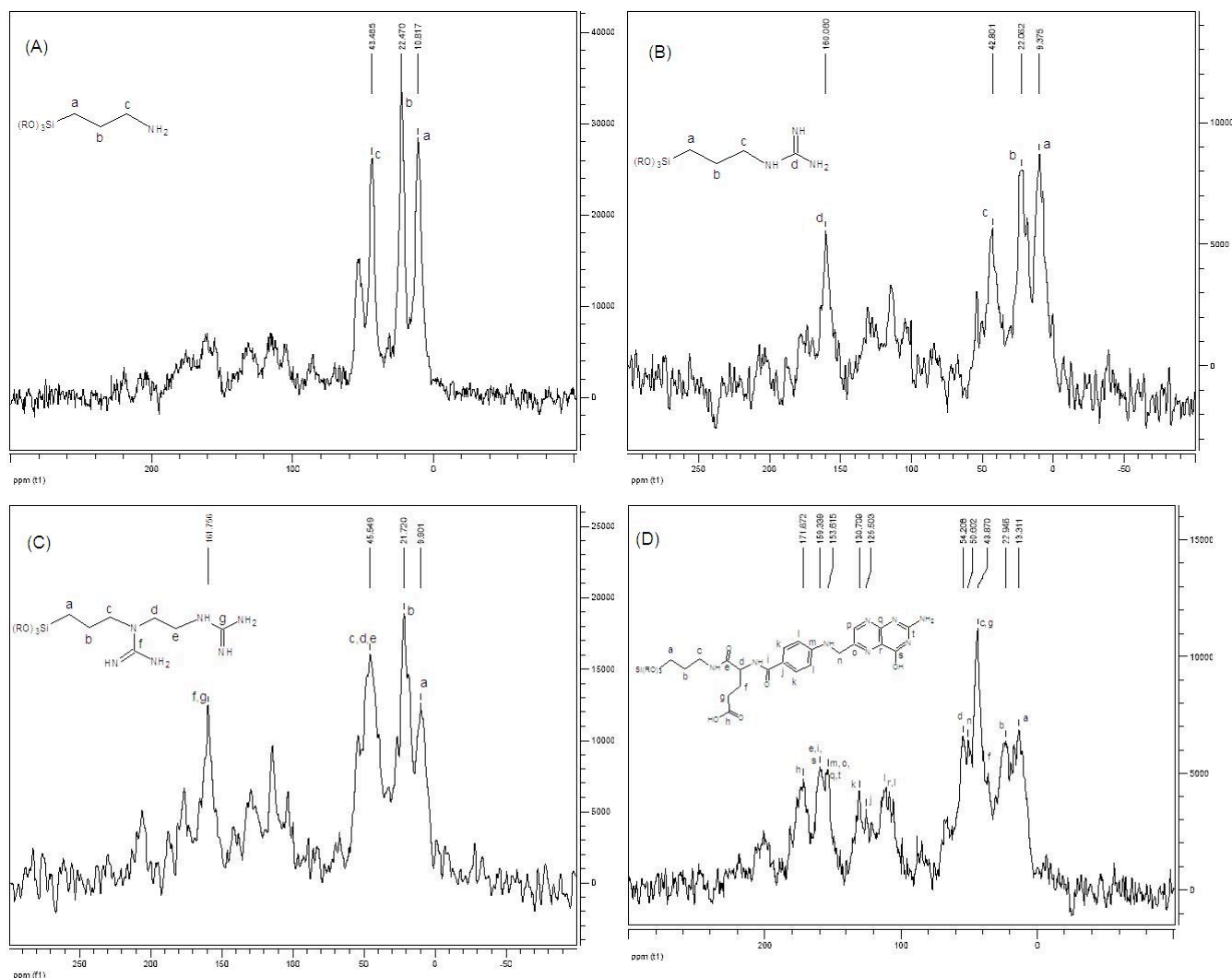


Figure S4. $^1\text{H} \rightarrow ^{13}\text{C}$ cross polarization (CP) solid-state NMR spectra of the functionalized materials: (A) AP-MSN, (B) GP-MSN, (C) GEGP-MSN and (D) FAP-MSN.

All spectra showed a small signal around 50 ppm, which is due to surface-adsorbed methanol from the washings. The smaller signals between 80 and 160 ppm correspond to the co-condensed FITC-APTMS. The signals at 160 and 161 ppm in (B) and (C), respectively, correspond to the guanidine carbons. No peaks of residual CTAB surfactant were observed in these measurements.

2.4.2. MAS DP ^{29}Si -NMR

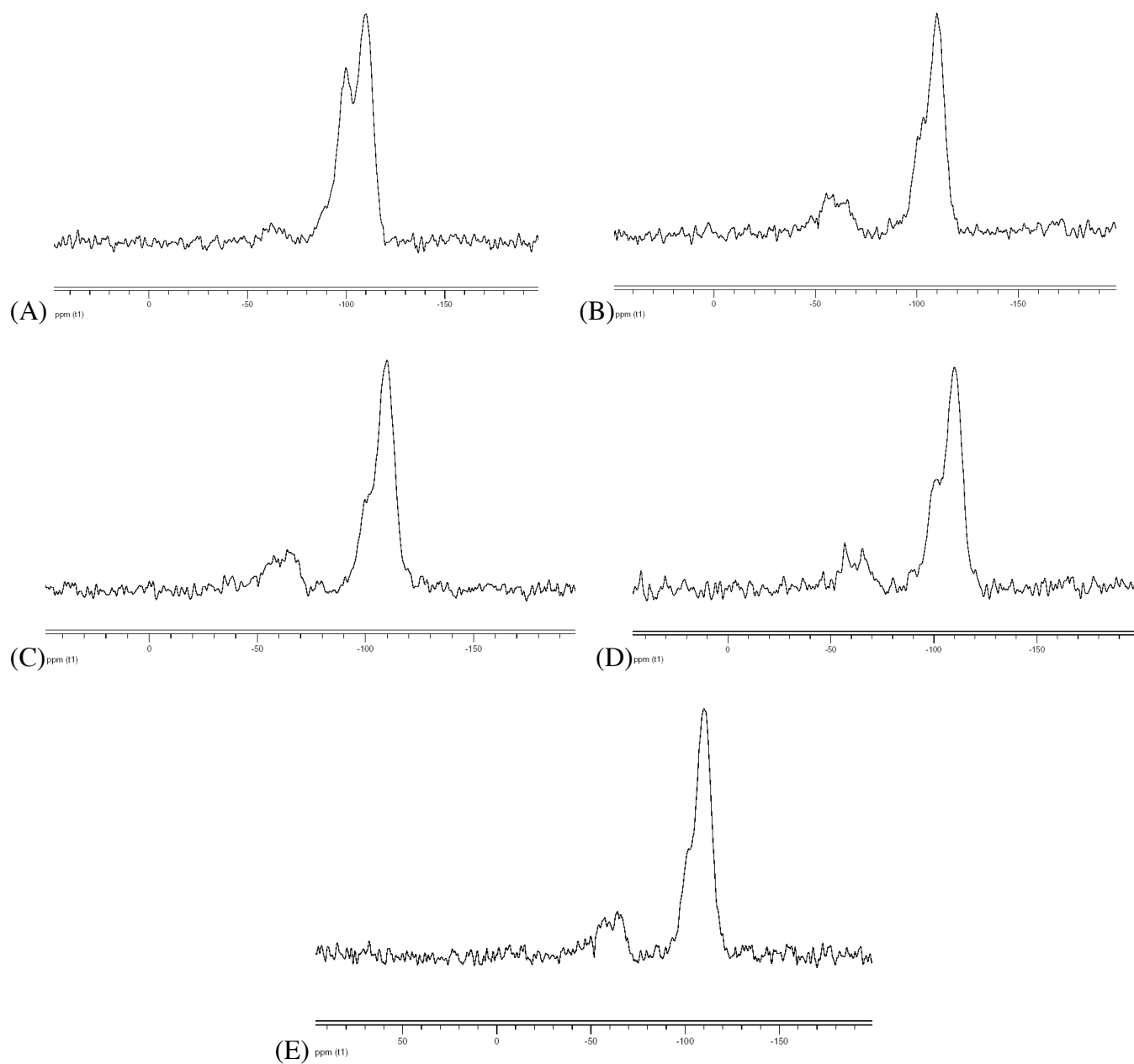


Figure S5. Direct polarization (DP) solid-state ^{29}Si -NMR spectra of all the materials: (A) FITC-MSN, (B) AP-MSN, (C) GP-MSN, (D) GEGP-MSN and (E) FAP-MSN.

Table S2. Composition of the materials as calculated from the DP ^{29}Si -NMR analysis.

| Material | Formula | Formula Mass | Loading [mmol/g] |
|----------|---|--------------|---------------------|
| FITC-MSN | $(\text{SiO}_2)_{100}(\text{H}_2\text{O})_{25}(\text{FITC}^*)_5$ | 8,691.2290 | 0.575 |
| AP-MSN | $(\text{SiO}_2)_{100}(\text{H}_2\text{O})_{13}(\text{FITC})_5(\text{C}_3\text{H}_6\text{NH}_2)_{14}$ | 9,288.4912 | 1.507 |
| GP-MSN | $(\text{SiO}_2)_{100}(\text{H}_2\text{O})_7(\text{FITC})_5(\text{C}_3\text{H}_6\text{NHC}(\text{NH})\text{NH}_2)_{13}$ | 9,668.8210 | 1.344 |
| GEGP-MSN | $(\text{SiO}_2)_{100}(\text{H}_2\text{O})_{12}(\text{FITC})_5(\text{C}_3\text{H}_6\text{N}(\text{CNHNH}_2)\text{C}_2\text{H}_4\text{NHC}(\text{NH})\text{NH}_2)_{10}$ | 10,309.5545 | 0.970 |
| FAP-MSN | $(\text{SiO}_2)_{100}(\text{H}_2\text{O})_5(\text{FITC})_5(\text{C}_3\text{H}_6\text{NHC}_{19}\text{H}_{18}\text{N}_7\text{O}_5)_{13}$ | 14,590.3118 | 0.891 |

* FITC = $\text{C}_3\text{H}_6\text{NHSC}_{21}\text{H}_{11}\text{NO}_5$

2.5. Scanning electron microscopy

Particle morphology was investigated by using a JEOL 840A scanning electron microscope with a 10 kV acceleration voltage.

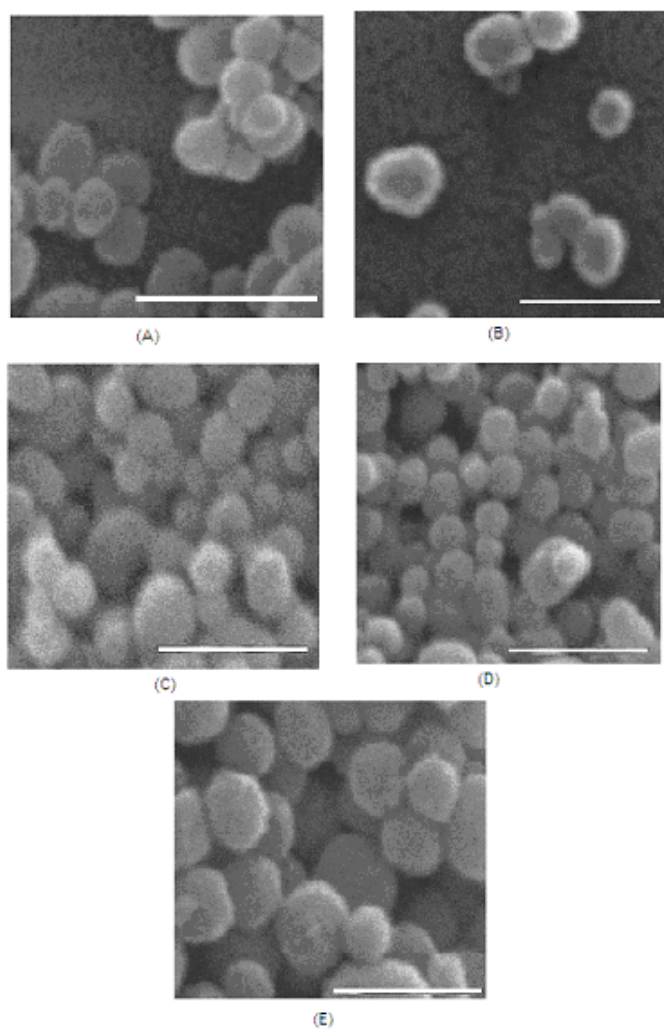


Figure S6. Scanning electron micrographs (SEMs) of (A) FITC-MSN, (B) AP-MSN, (C) GP-MSN, (D) GEGP-MSN, and (E) FAP-MSN. The scale bars are 500 nm. These materials are spherical particles ranging from 100 to 250 nm in diameter.

3. Measurement of uptake of the materials by HeLa Cells

The cellular uptake profiles of all MSNs were examined by FACS flow cytometry and fluorescence confocal microscopy.

3.1. Flow cytometry

For the flow cytometry assays, HeLa cells were seeded in six well plates with a density of 1×10^5 cells/mL in 3 mL of D-10 medium. The D-10 medium is a Dubelcco modified Eagle's medium (DMEM) containing 10% equine serum, *L*-alanylglutamine, gentamicin, and penicillin/streptomycin. After 34 h incubation, the D-10 medium was replaced by 3 mL of MSN suspensions at different concentrations ranging from 0.1 to 40 $\mu\text{g/mL}$ in the serum-free DMEM medium for 10 h. Different concentrations of MSN suspensions were tested. All the tests were run in triplicate. The cells were washed then with medium and harvested by trypsinization. After centrifugation the cell pellets were resuspended in 0.4 % trypan blue PBS solution, and analyzed by flow cytometry with a Becton-Dickinson FACSCanto cytometer and BD-FACS Diva software.

To distinguish the true fluorescence generated by the FITC-MSN from the natural autofluorescence of cells, a threshold of fluorescence intensity was established by performing the flow cytometry analysis on HeLa cells incubated without any MSN. The threshold was set at a fluorescence intensity slightly above the highest value observed for control samples (HeLa Cells only). The number of cells with encytosed MSNs was determined by counting the cells showing fluorescence intensity higher than the threshold.

3.2. Inhibition and competition assays

HeLa cells were seeded at the density of 1×10^5 cells/mL in 6 well plates and allowed to attach for 48 h in 3 mL of D-10 medium. The D-10 medium was then replaced by 3 mL of: (a) DMEM medium for the wells used as control, (b) 1 mM folic acid in DMEM medium for the wells used in the competition assay, and (c) 450 mM sucrose in DMEM medium for the wells used in the clathrin inhibition assay. The cells were left in contact with the media for 30 min. The media were then replaced with 3 mL of MSN (40 $\mu\text{g/mL}$) in: (a) DMEM medium for the control, (b) 1 mM folic acid in DMEM medium for the competition assay, and (c) 450 mM sucrose in DMEM medium for the clathrin inhibition assay. After 1 h, the cells were washed with DMEM medium and harvested by trypsinization. After centrifugation, the cell pellets were resuspended in 0.4% trypan blue PBS solution, and analyzed by flow cytometry with a Becton-Dickinson FACSCanto cytometer and BD-FACS Diva software.

3.3 Cell growth and viability assays

Cell growth and viability of the HeLa cells in the presence and absence of MSN were studied by Guava ViaCount assay (Guava Technologies, Inc.; Hayward, CA). For that purpose HeLa cells were seeded in four six well plates with a density of 1×10^5 cells/mL in 3 mL of D-10 medium containing (a) no MSNs, (b) FITC-MSN, (c) AP-MSN, (d) GP-MSN, (e) GEGP-MSN and (f) FAP-MSN. The concentration of the MSNs in the culture media was $40 \mu\text{g/mL}$. After seeding them the plates were set in an incubator at 37°C and $5\% \text{ CO}_2$ and every other day, for a lapse of four days, one plate was removed from the incubator, the media of each well was discarded, each well was washed with fresh D-10 medium and the cells trypsinized, centrifuged and resuspended in D-10 medium. The cells in the resuspended media were then counted and their viability determined by the Guava ViaCount cytometry assay. Figure S7 shows the results of the cell counts at every day, the viability was found to be between 90 and 100 %.

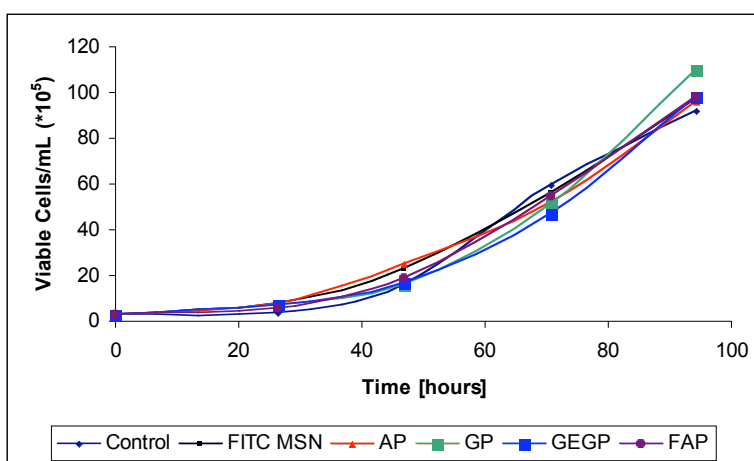


Figure S7. Cell counts performed with Guava ViaCount assay after incubation at different times in absence and in presence of $40 \mu\text{g/mL}$ of the MSNs in D-10 media.

3.4. Confocal fluorescence microscopy

3.4.1. Localization of the MSNs inside the cells

For confocal fluorescence microscopy measurements, HeLa cells were seeded at the density of 1×10^5 cells per well in 6 well plates in 3 mL D-10 medium with coverslips at the bottom of the wells. After 34 h incubation, the D-10 medium was replaced by 3 mL of MSNs ($40 \mu\text{g/mL}$) in the serum-free DMEM medium for 10 h. The cell-plated coverslips were then washed with medium and soaked for 30 min in 3 mL of 0.4 % trypan blue in 100 mM PBS buffer (pH 7.4). The trypan blue solution was then replaced by a solution of $5.7 \mu\text{M}$ 4',6-Diamidino-2-phenylindole (DAPI) and 3.7 % formaldehyde in 100 mM PBS buffer pH 7.44. The DAPI-stained coverslips were placed in microscope slides and examined under a Leica TCS NT confocal fluorescence microscope system using a 100x oil immersion objective. As depicted in Figure S8, the blue fluorescent, DAPI-stained nuclei (right images) were clearly observed by exciting the cells with a UV laser at wavelengths from 340 to 458 nm. The green fluorescent FITC-MSN particles inside of the HeLa cells (middle images) were visualized by excitation at 488nm with an Argon Laser and the phase contrast images of the cells (left images) were obtained with a 568nm Krypton laser.

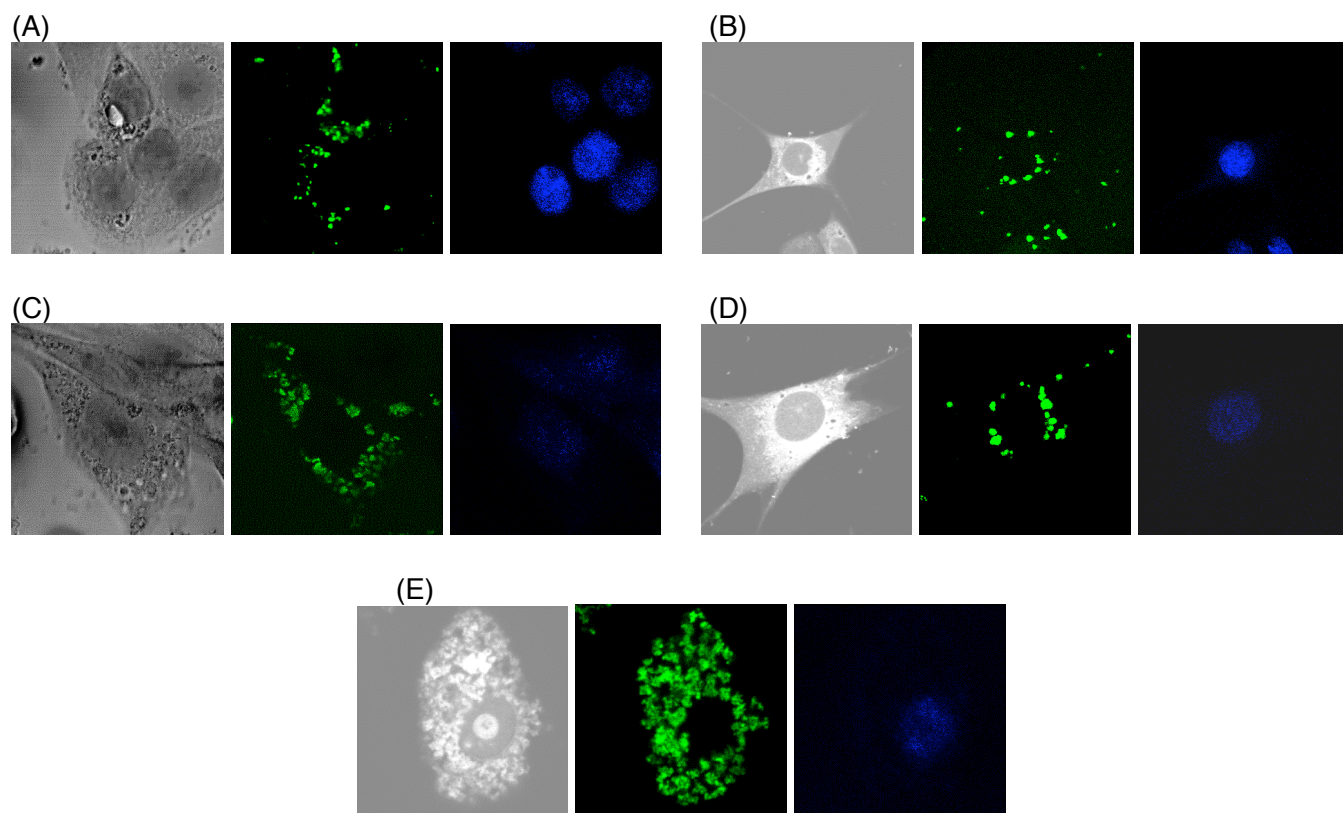


Figure S8. Confocal fluorescence images of HeLa cells loaded with the different organically functionalized MSNs: (A) FITC-MSN, (B) AP-MSN, (C) GP-MSN, (D) GEGP-MSN, and (E) FAP-MSN. The left images were taken with a Krypton laser source, the ones in the middle showed the endocytosed green fluorescent FITC-labeled MSN particles (Argon laser) and the right images exhibited the blue fluorescent, DAPI-stained nuclei (UV laser).

3.4.2. Localization of the MSNs inside the cells in presence of an endosome marker

HeLa cells were seeded at the density of 1×10^5 cells per well in 6 well plates in 3 mL D-10 medium with coverslips at the bottom of the wells. After 38 h incubation, the D-10 medium was replaced by 3 mL serum-free DMEM medium containing MSNs (40 $\mu\text{g/mL}$) and the endosome marker FM 4-64 (10 $\mu\text{g/mL}$) and incubated for 6 h. The cell-plated coverslips were then washed with medium and soaked for 30 min in 3 mL of 0.4 % trypan blue in 100 mM PBS buffer (pH 7.4). The trypan blue solution was then replaced by a solution of 5.7 μM 4',6-Diamidino-2-phenylindole (DAPI) and 3.7 % formaldehyde in 100 mM PBS buffer pH 7.44. The DAPI-stained coverslips were placed in microscope slides and examined under a Leica TCS NT confocal fluorescence microscope system using a 100x oil immersion objective. Both, the MSNs and the endosome marker were excited at 488 nm with an Argon Laser, the MSNs were detected at wavelengths in the 515 to 590 nm range (observed green) while the endosome marker was detected at wavelengths in the 590 to 750 nm range (observed red). MSNs are considered to be inside of the endosomes in the spots where the green and the red spots are co-localized to give a yellow color. The phase contrast images of the cells (right images) were obtained with a 568nm Krypton laser.

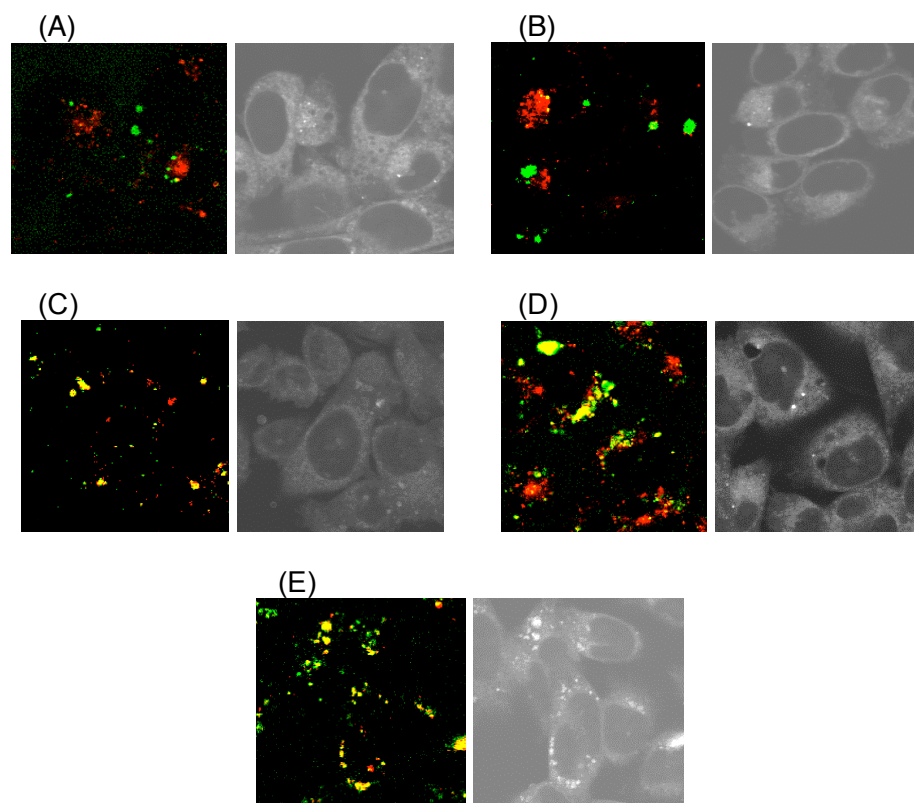


Figure S9. Confocal fluorescence images of HeLa cells loaded with the different organically functionalized MSNs: (A) FITC-MSN, (B) AP-MSN, (C) GP-MSN, (D) GEGP-MSN, and (E) FAP-MSN, and stained with the endosome marker FM 4-64. The images to the right were taken with a Krypton laser source, and the ones to the left show the Argon laser excited endocytosed green fluorescent FITC-labeled MSNs, the red fluorescent marked endosomes, and the yellow spots where the MSNs and endosomes are colocalized.